

Atomic structure model of the reconstructed Si(557) surface with a triple step structure: Adatom-parallel dimer model

D.-H. Oh,^{1,*} M. K. Kim,^{1,2} J. H. Nam,^{1,2} I. Song,^{1,2} C.-Y. Park,^{1,2,3} S. H. Woo,⁴ H.-N. Hwang,⁵
C. C. Hwang,⁵ and J. R. Ahn^{1,2,3,†}

¹*BK21 Physics Research Division, Sungkyunkwan University, 300 Cheoncheon-dong, Jangan-gu, Suwon 440-746, Republic of Korea*

²*Center for Nanotubes and Nanostructured Composites (CNNC), Sungkyunkwan University, 300 Cheoncheon-dong, Jangan-gu, Suwon 440-746, Republic of Korea*

³*SKKU Advanced Institute of Technology (SAINT), Sungkyunkwan University, 300 Cheoncheon-dong, Jangan-gu, Suwon 440-746, Republic of Korea*

⁴*College of Pharmacy, Chungnam National University, Daejeon 305-764, Republic of Korea*

⁵*Pohang Accelerator Laboratory, San 31, Hyoja-dong, Pohang 790-784, Republic of Korea*

(Received 16 November 2007; revised manuscript received 26 January 2008; published 18 April 2008)

We studied the atomic and electronic structures of the reconstructed Si(557) surface composed of one (111) facet and three (112) facets in its single unit cell by using first principles calculations, scanning tunneling microscopy, and angle-resolved photoemission spectroscopy. A variety of atomic structure models of the (112) facet were introduced to understand overall properties of the Si(557) surface. Among the atomic structure models considered, an adatom-parallel dimer model with a missing dimer with the same bonding network as the Si(111)-7×7 surface was found to be the most stable model. The scanning tunneling microscopy images and photoemission spectra of the Si(557) surface can be widely explained by the model. In addition, these results suggest that the (112) facet with a width of 0.9 nm can be used as a one-dimensional template, as the Si(111)-7×7 surface plays the role of a two-dimensional template for various quantum dot arrays.

DOI: [10.1103/PhysRevB.77.155430](https://doi.org/10.1103/PhysRevB.77.155430)

PACS number(s): 68.35.B-, 68.47.Fg, 71.15.Nc, 68.37.Ef

I. INTRODUCTION

One-dimensional (1D) exotic phenomena such as Tomonaga–Luttinger liquid and Peierls instability have become a subject of intense research because of the fabrication of 1D electron systems.^{1–3} However, few 1D structures have been assembled on surfaces because of a variety of parameters, such as the surface orientation of a substrate, the type and coverage of an adsorbate, and temperature, which need to be satisfied in order to grow anisotropic structures. For example, the Si honeycomb chain channel on the metal/Si(111)-3×1 surface,⁴ the zigzag In chain on the In/Si(111)-4×1 surface,⁵ and the Si double honeycomb chain on the Au/Si(111)-5×1 surface⁶ have been reported.

Recently, vicinal Si(111) surfaces, which are represented by Si(557) and Si(553), have been considered to fabricate 1D structures because of their anisotropic structures.^{7–13} The anisotropic structures of vicinal surfaces minimize the number and range of parameters that need to be adjusted in the growth of a 1D structure. In addition, their step edges reduce the coherence between 1D structures on different terraces and, consequently, confine electrons within a terrace. The strong points of vicinal surfaces were demonstrated by using the two representative Au/Si(557) and Au/Si(553) surfaces with multiple 1D energy bands.^{7,8,10,11} The 1D energy bands produce interesting 1D phenomena, such as the Peierls instability on the Au/Si(557) surface,⁷ the coexistence of ×2 and ×3 Peierls distortions on the Au/Si(553) surface,⁸ and spin-orbit-split 1D metallic bands.¹² More recently, switching between one and two dimensions in conductivity was observed on the Pb/Si(557) surface.¹³

One excellent method using vicinal Si(111) surfaces as a 1D template is to grow a 1D structure, while keeping the

overall geometries of their clean surfaces. For self-assembled quantum dots, it was demonstrated that a variety of metal quantum dots can be assembled while maintaining the overall structure of the Si(111)-7×7 surface.¹⁴ Among the vicinal Si(111) surfaces, only the Si(557) surface was found to have a regular 1D structure with the alternative arrangement of one (111) facet with atomic rows of 9 and three (112) facets with atomic rows of 2²/3.¹⁵ In addition, the (112) facet has the smallest terrace width ever found among the vicinal Si(111) surfaces and can be a 1D template with the smallest width. However, the atomic structure of the (112) facet is still unknown. Therefore, it is important to understand the atomic structure of the (112) facet. This can lead to an understanding of the entire structure of the Si(557) surface.

In this study, we considered five atomic structure models of the (112) facet. The bulk-terminated Si(112)-1×1 structure was used as a foundation. Adatoms and dimers were introduced to the 1×1 structure. Among the atomic structure models that are examined, an atomic structure model with an adatom within the terrace and a parallel dimer at the step edge was found to be the most stable model. This is called the adatom-parallel dimer model. To explain the scanning tunneling microscopy (STM) image with a ×7 order along the step edge direction of the Si(112) facet, every fourth dimer on the model was removed. The removal resulted in a structure similar to the corner hole of the Si(111)-7×7 surface.¹⁶ Based on the modified adatom-parallel dimer model, the two rows of bright protrusions of the STM image of the (112) facet were successfully reproduced by its simulated STM image and the origins of the two surface states with small band widths of the Si(557) surface were disclosed.

II. METHOD

First principles calculations were performed by using VASP,¹⁷ which is a plane-wave-pseudopotential code based on density functional theory. The electron-electron and electron-ion potentials were described by a local density approximation¹⁸ and a projected augmented wave method,¹⁹ respectively. Electronic wave functions were expanded by plane waves up to a kinetic energy cutoff of 250 eV. The pseudopotentials were generated to fit enough atomic wave functions, atomic energy eigenvalues, and scattering properties of all electron calculations. A slab geometry in an orthorhombic unit cell was used to describe the (112) facet, where the surface area was 31.2 \AA^2 for the 1×1 unit cell. This unit cell contains three Si bilayers, and Si atoms at the bottom were saturated by hydrogen. A vacuum region of approximately 14 \AA was used. For the \vec{k} -point sampling, 7×3 , 4×3 , and 1×3 Monkhorst–Pack meshes²⁰ were used for the 1×1 , 2×1 , and 7×1 unit cells in the surface Brillouin zone, respectively. A combination of quenched dynamics and quasi-Newtonian methods was used for structural relaxation. The criterion of force for this was $2.0 \times 10^{-2} \text{ eV/\AA}$. The conditions for the theoretical calculations were confirmed using convergence tests for the kinetic energy cutoff, the \vec{k} -point sampling, and the number of atomic layers in the slab. For example, the convergence for the relaxed bulk-terminated (RBT) model was described in the following. The total energies were changed to 0.01% and 0.1%, when 1% and 10% larger than the kinetic energy cutoff of 250 eV were used, respectively. For the \vec{k} -point sampling, the total energy in the case of the 7×3 Monkhorst–Pack mesh was 0.06% larger than in the case of the 5×3 Monkhorst–Pack mesh. In addition, the same densities as the \vec{k} -point sampling were used for other structure models. Mankefors *et al.*²¹ demonstrated that eight layers, which are equal to the three bilayers in this study, for the RBT model is sufficient for calculating the surface energy. A simulated STM image was calculated by utilizing the method proposed by Tersoff and Hamann.²²

Angle-resolved photoemission spectra were measured at a vacuum ultraviolet beamline (BL-3A2) connected to an undulator of the synchrotron radiation source at the Pohang Light Source (PAL) in Korea. The end station is equipped with a high-resolution electron analyzer (SES-R4000, Gamma Data, Sweden). The nominal energy and angle resolutions were better than 40 meV and 0.15° , respectively. A commercial variable-temperature STM (Omicron, Germany) was used. A *n*-type phosphorus-doped Si(557) wafer with resistivity of $1 \text{ } \Omega \text{ cm}$ was used. The Si(557) substrate (9.45° offcut from the $[111]$ orientation) was thermally cleaned. The electric voltage for the thermal treatment was applied along the step edge direction.¹⁵

III. RESULTS AND DISCUSSION

A. Experimental data

Figure 1 shows a STM image of the reconstructed Si(557) surface. The bulk-terminated Si(557)- 1×1 structure has atomic rows of $5\frac{2}{3}$ and a width of 1.92 nm, as shown in Fig. 1(c). The reconstructed surface has a larger unit cell

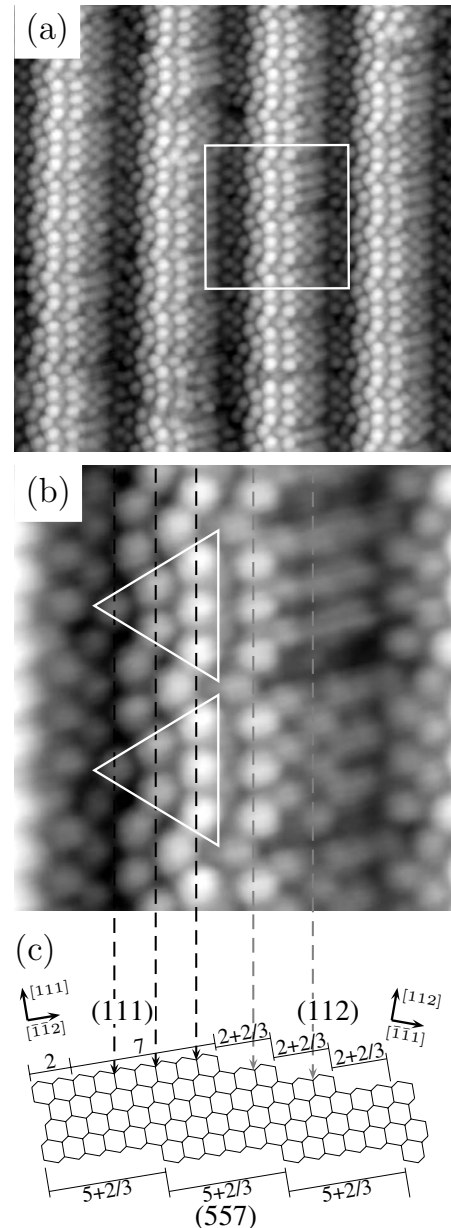


FIG. 1. (a) An empty-state STM image of the Si(557) surface acquired with a bias voltage of 1.0 V, (b) the enlarged STM image of the white rectangle region in (a), and (c) the bulk-terminated 1×1 structure of the Si(557) surface, which was proposed by Kirakosian *et al.* (Ref. 15). The white triangle is the half unit cell of the 7×7 structure on the (111) facet and the black and gray dotted arrows are drawn as a guide.

with a width of 5.73 nm, which is equal to atomic rows of $3 \times 5\frac{2}{3}$. Kirakosian *et al.*¹⁵ suggested that the larger unit cell of the reconstructed surface consists of the alternative order of a single (111) facet with atomic rows of 9 and three (112) facets with atomic rows of $2\frac{2}{3}$. The triple step structure has been observed on vicinal Si(111) surfaces with a miscut toward the $[\bar{1}\bar{1}2]$ direction.^{23–25} In addition, the (111) facet was suggested to have the same surface reconstruction as the Si(111)- 7×7 surface.¹⁵ This is because the STM image of the dimer-adatom-stacking fault (DAS) structure of

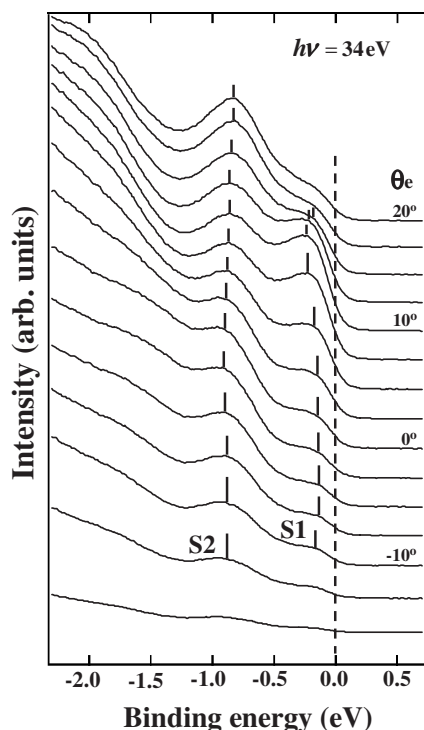


FIG. 2. Photoemission spectra of the Si(557) surface along the step edge direction measured with a photon energy of 34 eV, where θ_e is the emission angle.

the Si(111)- 7×7 surface was reported to be identical to that of the (111) facet, as indicated by the triangle in Fig. 1.¹⁵

However, the atomic arrangement of the entire Si(557) surface is still unknown. In the STM images that were previously reported,^{26–28} only the (111) facet was imaged with atomic resolution but the (112) facets were not visualized clearly because of their narrow widths. In this study, the atomic protrusions of the (112) facets were successfully imaged, as shown in Fig. 1. The (112) facet had a $\times 7$ order along the step edge direction and was composed of two rows of bright protrusions that were located at the step edge and within the terrace. Their relative intensities with respect to each other depended on the locations of the three (112) facets. The protrusion chain within the terrace on the first (112) facet was brighter than that at the step edge. However, on the second (112) facet, the brightness of the terrace protrusions was similar to that of the step edge protrusions. This does not mean that the two (112) facets have different atomic arrangements. This is partly because it is more difficult for a STM tip to approach a lower (112) facet. Although only the $\times 7$ period was observed in these STM images, previous low energy electron diffraction studies reported a $\times 2$ period along the step edge direction in addition to the $\times 7$ period.^{29,30} This will also be discussed based on the following theoretical calculations. The reconstructed Si(557) structure was further studied by angle-resolved photoemission spectroscopy. Figure 2 shows the valence band spectra of the Si(557) surface. Two surface states were found to be located at a binding energy (BE) of 0.15 (S1) and 0.9 eV (S2) at the normal emission, as recently reported.²⁸ In a previous report, only the valence band spectrum at the normal emission was

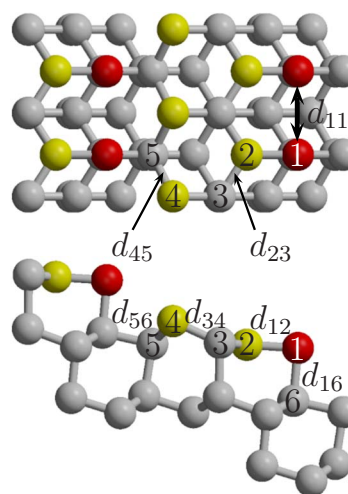


FIG. 3. (Color online) The top and side views of the RBT model, where the red (atom 1, dark gray) and yellow (atoms 2 and 4, light gray) balls indicate the 2FC and 3FC Si atoms, respectively.

measured. In this study, the extended valence band spectra were measured along the step edge direction in order to determine the energy dispersion of the two surface states. The two surface bands were found to be flat with a bandwidth of < 0.1 eV. The characteristics of the two surface states are quite similar to those of the Si(111)- 7×7 surface. The Si(111)- 7×7 surface has three surface states with BEs of 0.15, 0.5, and 0.9 eV with small bandwidths of < 0.1 eV, which originate from the center adatoms, corner adatoms, and restatoms, respectively.³¹ This suggests that, in addition to the (111) facet, the (112) facet may have a similar atomic structure to that of the Si(111)- 7×7 surface.

B. Atomic structure models of the (112) facet

Various atomic structure models of the (112) facet were examined by using first principles calculations to highlight the detailed atomic geometry of the (112) facet. Figure 3 shows the RBT model, which was obtained by using a total energy minimization scheme, as described in Sec. II. The twofold-coordinated (2FC) atom 1 is located at the step edge and the threefold-coordinated (3FC) atoms 2 and 4 are located within the terrace. Atoms 2 and 4 move downward along the $[\bar{1}\bar{1}\bar{1}]$ direction by 0.75 and 0.11 Å, respectively, in order to relax the surface tension. Atom 2 can easily push out atom 1 so that atom 2 moves downward much more than atom 4. This results in a flat structure at the step edge. The two dangling bonds of the 2FC atom make the RBT model energetically unstable and leave a margin for additional energy minimization. There are two ways to decrease the number of dangling bonds. One is to remove atom 1 at the step edge and make a 2-6 dimer.^{32,33} The other is that the neighboring two atoms form a dimer.^{32,33} The former is the perpendicular dimer (D_{\perp}) model and the latter is the parallel dimer (D_{\parallel}) model [see Figs. 4(a) and 4(b), respectively].

The D_{\perp} geometry was generated by using the following sequence. First, the 2FC atom 1 in the RBT model was removed. Second, a total energy minimization scheme was car-

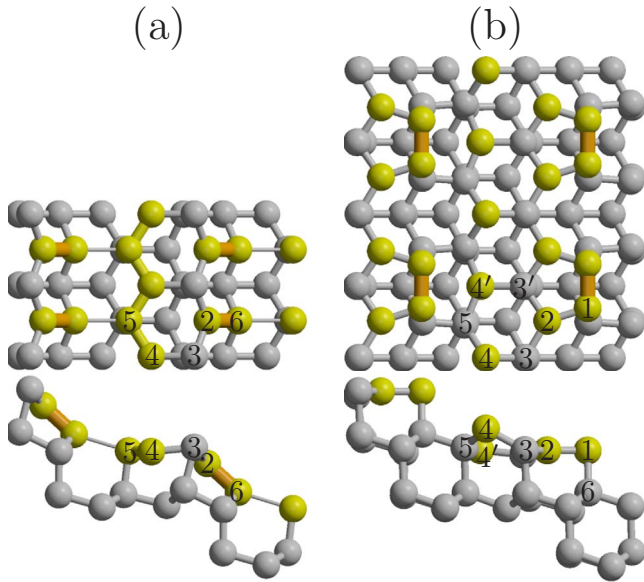


FIG. 4. (Color online) The top and side views of the (a) D_{\perp} and (b) D_{\parallel} models. The yellow ball [atoms 2, 4, 5, and 6, light gray balls in (a) and atoms 1, 2, 4, and 4', light gray balls in (b)] indicates a 3FC Si atom and the thick orange (light gray) cylinder indicates a dimer. The yellow (4-5, light gray) cylinder in (a) indicates a π -bonded chain.

ried out to make a 2-6 dimer, as shown in Fig. 4(a). The resulting 2-6 dimer with a bond length of 2.50 Å, which is perpendicular to the step edge, saturated the dangling bonds that were generated after removing atom 1. This is similar to the dimer of the Si(100)- 2×1 surface.³⁴ The dimer formation broke the 5-6 bond and left a dangling bond on atom 5. This results in a π -bonded chain along the zigzag 4-5 chain with a bond length of 2.28 Å, which resembles Pandey's model of the Si(111)- 2×1 surface.³⁵ The relative energy gain from the dimerization and π -bonded chain formation to the RBT geometry was 0.54 eV/ 1×1 . Here, the surface energy was calculated by using the following equation:³²

$$E_{\text{surf}} = E_{\text{tot}} - N_{\text{Si}} E_{\text{bulk}}, \quad (1)$$

where E_{tot} is the total energy of the model, N_{Si} is the number of Si atoms in the model, and E_{bulk} is the energy of a bulk Si atom.

There is another way to decrease the number of dangling bonds of the 2FC atom. As described above, this way is to make the D_{\parallel} geometry, where adjacent 2FC atoms in the RBT model form a dimer which is parallel to the step edge, as shown in Fig. 4(b). The bond length of the dimer is 2.41 Å, which is shorter than that of the D_{\perp} model. This induces a $\times 2$ lattice modulation along the step edge direction of atom 4 on the RBT model. Atom 4' in the D_{\parallel} model was lowered by 0.58 Å and atom 4 was raised by 0.35 Å. The energy gain on account of the dimerization was 0.51 eV/ 1×1 . Therefore, the D_{\perp} model is slightly more energetically stable than the D_{\parallel} model.

However, this does not mean that the perpendicular dimer on the reconstructed Si(557) surface is more favored than the parallel dimer. This is because the D_{\parallel} geometry has a margin

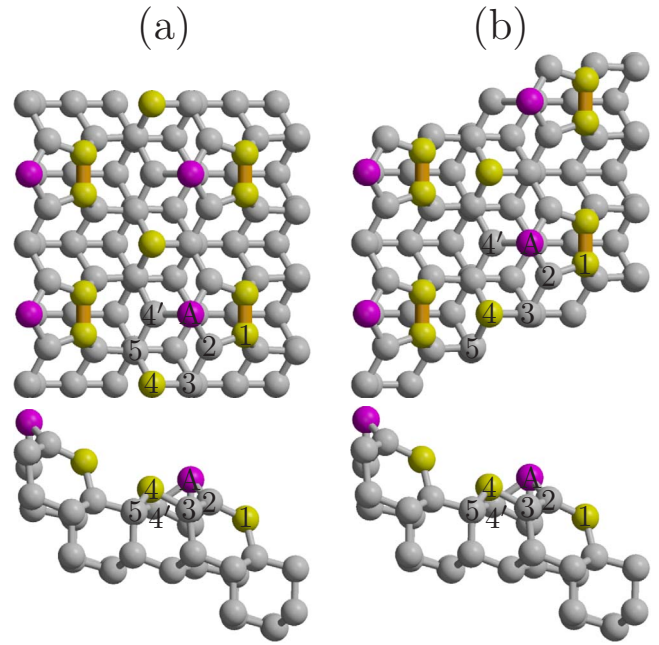


FIG. 5. (Color online) The top and side views of the adatom-parallel dimer models with (a) normal (AD_{\parallel}) and (b) oblique orientations (AD'_{\parallel}), where an adatom is denoted by the magenta (dark gray) ball.

for further energy reductions. The dangling bonds of the 3FC Si atoms within the terrace can be saturated by introducing an additional adatom, which is called the AD_{\parallel} model, as shown in Fig. 5(a). Here the adatom, denoted by A, raised atoms 2 and 4, which drew the parallel dimer toward the terrace. The relative energy gain due to the introduction of the adatom to the D_{\parallel} model was 1.1 eV/ 1×1 . This suggests that the AD_{\parallel} model is the most stable model among the models considered above. The AD_{\parallel} model is quite similar to the DAS model of the Si(111)- 7×7 surface.¹⁶ The structure similarity suggests that atom 4 with 3FC corresponds to the restatom of the DAS model. A further energy reduction can be considered. There are two different types of arrangements of the parallel dimer across the step edge direction. One is to locate the parallel dimer at the same site on all step edges, which is identical to the AD_{\parallel} model that is described above. Another is to make the site of the parallel dimer shift alternatively across the step edge direction. This is called the AD'_{\parallel} geometry, as shown in Fig. 5(b). This oblique configuration of the parallel dimer results in a further energy gain of 0.14 eV/ 1×1 , which is on account of surface stress relief by the oblique configuration. (Table I)

C. Comparisons of the atomic structure models to experimental data

The AD_{\parallel} and AD'_{\parallel} models need to be modified in order to construct a suitable structure model, which matches the STM image and valence band structure of the reconstructed Si(557) surface. The STM image of the Si(557) surface shows that the (112) facet has a $\times 7$ order along the step edge direction similar to the Si(111)- 7×7 surface, as shown in Fig. 1(a). However, the AD_{\parallel} and AD'_{\parallel} geometries have a $\times 2$

TABLE I. Summary of the geometries and energetics of the structure models of the (112) facet. Here, d_{nm} indicates the distance between n and m Si atoms, as illustrated in Fig. 3. ΔE_{surf} is the relative surface energy per 1×1 unit cell to the RBT model. The unit of d_{nm} is Å.

	RBT	D_{\perp}	D_{\parallel}	AD_{\parallel}	AD'_{\parallel}
d_{11}	3.84		2.36	2.22	2.25
d_{12}	2.38		2.26	2.29	2.30
d_{16}	2.44		2.35	2.32	2.34
$d_{23}, d_{23'}$	2.29	-2.22	-2.31, 2.27	2.37, 2.38	2.38, 2.41
$d_{34}, d_{3'4'}$	2.39	-2.33	-2.37, 2.30	2.34, 2.30	2.38, 2.27
$d_{45}, d_{4'5'}$	2.39	-2.28	-2.34, 2.24	2.36, 2.31	2.38, 2.32
d_{26}	3.36	2.29	3.14	3.98	3.96
d_{56}	2.38	3.08	2.38	2.33	2.32
d_{A2}				2.40	2.39
d_{A3}				2.43	2.46
d_{A4}				2.46	2.50
ΔE_{surf} (eV)	0.00	-0.54	-0.51	-0.62	-0.76

order along the step edge direction. Therefore, the AD_{\parallel} and AD'_{\parallel} models need to be modified to reproduce the STM image. The AD_{\parallel} and AD'_{\parallel} models have the same local atomic structure as the DAS model of the Si(111)- 7×7 surface. In addition, the STM image of the (112) facet is quite similar to that of the Si(111)- 7×7 surface. This suggests that the dark site near the three bright protrusions along the step edge in the STM image can be produced by a structure similar to the corner hole of the DAS model. Initially, the 1×1 structure of the RBT model was inserted at every fourth parallel dimer site. Subsequently, atoms 1 and 2 were removed from the 1×1 structure. This makes atoms 3 and 6 become 2FC. An additional adatom on atom 5 was then introduced to saturate the dangling bonds of atoms 4 and 6. The resulting structure constructed through this process is similar to the corner hole of the DAS model, as shown in Fig. 6. The energy gain from the modification was 0.06 eV/ 1×1 .

The simulated STM image of the modified AD_{\parallel} model was generated, as shown in Fig. 6, where an energy window of $[E_{\text{Fermi}}, E_{\text{Fermi}} + 1 \text{ eV}]$ was used. The simulated STM image shows that the adatoms near the parallel dimer produce brighter protrusions and the adatoms near the corner hole generate darker protrusions. Furthermore, the corner holes were appeared dark. Hence, the simulated STM image reproduces the experimental STM image successfully. On the other hand, it may be due to the limited spatial resolution that the dumbbell image of the dimer in the simulated STM image is shown as a protrusion in the experimental STM image. The upper part at the lower (112) facet of the experimental STM image in Fig. 1(b) shows that the bright protrusions are differently located. This can be explained by the coexistence of the AD_{\parallel} and AD'_{\parallel} geometries due to the small energy difference.

The validity of the modified AD_{\parallel} and AD'_{\parallel} models require further confirmation by comparing their electronic structures with the experimental valence band structure of the Si(557) surface. Figure 7(a) shows the electronic density of state (DOS) at $\bar{\Gamma}$ of the AD_{\parallel} model. Here, only the AD_{\parallel} model is considered because the AD_{\parallel} and AD'_{\parallel} models are similar.

The Si(557) surface is composed of (111) and (112) facets, as described above. The (111) facet is almost identical to the Si(111)- 7×7 surface. The (111) facet is thus expected to

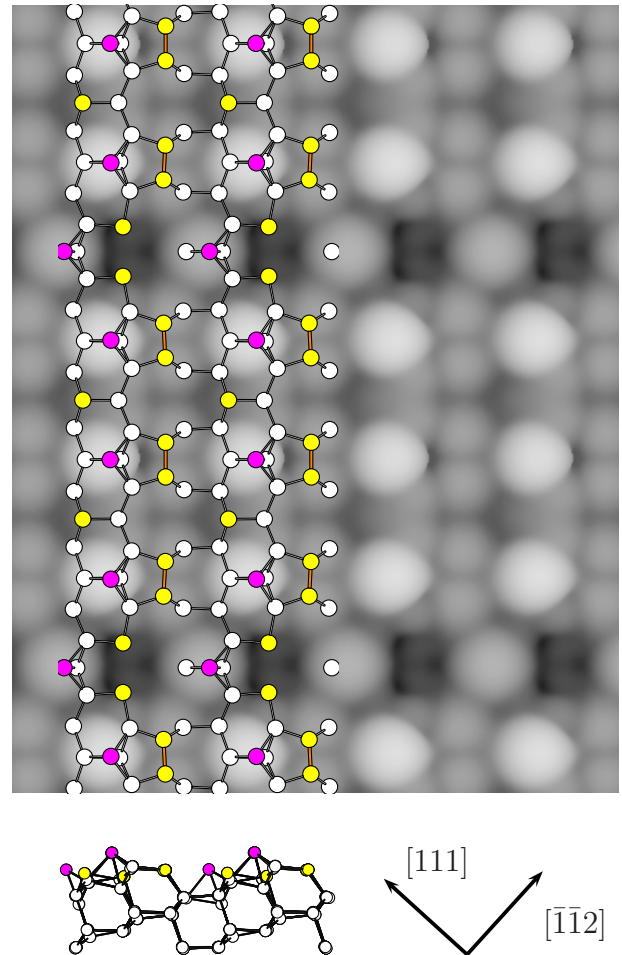


FIG. 6. (Color online) The top and side views of the AD_{\parallel} model with a missing dimer and its simulated STM image acquired using an energy window of $[E_{\text{Fermi}}, E_{\text{Fermi}} + 1 \text{ eV}]$.

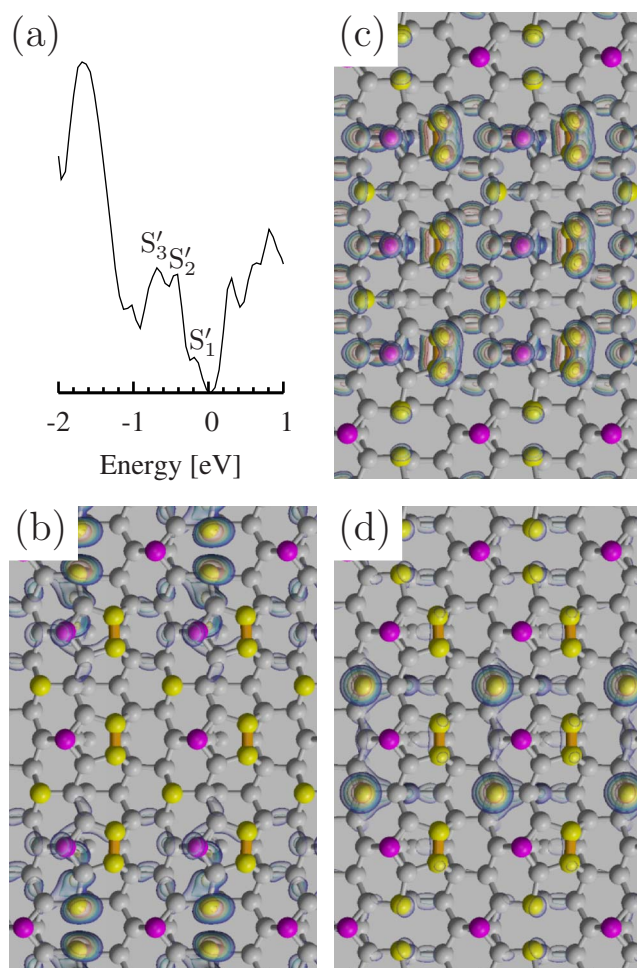


FIG. 7. (Color online) (a) The electronic density of states at $\bar{\Gamma}$ of the $AD_{||}$ model with a missing dimer. Selected probability densities of an electron with energy windows near the (b) S'_1 , (c) S'_2 , and (d) S'_3 states. The electron density is drawn by a nested equidensity surface with a rainbow (gray) scale: a higher equidensity surface is drawn by a red (light gray) surface and a lower equidensity surface is drawn by a blue (dark gray) surface.

produce the same surface states as the $Si(111)-7 \times 7$ surface, whose three surface states are located at BEs of 0.15, 0.5, and 0.9 eV, respectively.³¹ The DOS of the $AD_{||}$ model of the (112) facet reveals three surface states to be located at BEs of 0.18 (S'_1), 0.4 (S'_2), and 0.7 eV (S'_3). Figures 7(b)–7(d) show the origins of the three surface states. This suggests that the S'_1 , S'_2 , and S'_3 states mainly originate from the corner hole atoms, dimers, and adatoms, respectively. The electron density of the surface states are spatially localized so that their energy dispersion can be quite flat along the step edge direction. This suggests that the number of the surface states of the (112) facet is identical to that of the (111) facet and the BEs of the surface states of the (112) and (111) facets are quite similar, even though the surface states of the (112) and (111) facets have different origins. The similarity explains enough how the valence band structure of the $Si(557)$ surface can be similar to that of the $Si(111)-7 \times 7$ surface. These results also suggest that the S_1 state originates from the corner hole atoms on the (112) facet and the adatoms on

the (111) facet. Moreover, the S_2 state is produced by the adatoms on the (112) facet and the restatoms on the (111) facet. The reason why the surface states near a BE of 0.5 eV were not well resolved in the photoemission spectra may be partly because the surface states originating from the (111) and (112) facets overlap. Our theoretical calculations could also explain the $\times 2$ period observed in the low energy electron diffraction pattern. The energy difference between the $AD_{||}$ model with the $\times 2$ period and the modified $AD_{||}$ model with the $\times 7$ period was 0.06 eV/ 1×1 . This small energy difference suggests that the $AD_{||}$ structure with the $\times 2$ period can be produced on the (112) facet under a thermal treatment condition. Another possible scenario is that a structure with a $\times 2$ period is made on a separate facet from the $Si(557)$ surface because most of the $Si(557)$ wafers have small off-angles from an ideal $Si(557)$ surface.

The experimental data are successfully explained by our structure models, but there are still some problems remaining. There was insufficient computing power to calculate the surface energy of the whole structure of the reconstructed $Si(557)$ surface because the $Si(557)$ surface has a large unit cell of 17×7 if a bulk-terminated $Si(111)-1 \times 1$ structure is considered to be a 1×1 unit cell. This leaves some unanswered questions regarding the $Si(557)$ surface. One question is why the $Si(557)$ surface with one (111) and two (112) facets is energetically stable. Another is why the surface energies of the structure models of the (112) facet considered in this study can be changed slightly after connecting the (112) facet with the (111) facet to construct the whole $Si(557)$ structure. These issues need to be examined in future studies.

IV. CONCLUSION

The atomic and electronic structures of the reconstructed $Si(557)$ surface were investigated by using the combined approach of first principles calculations, STM, and angle-resolved photoemission spectroscopy. The overall properties of the $Si(557)$ surface composed of the (111) and (112) facets were unveiled by testing various atomic structure models of the (112) facet relatively with a lack of information. Among the various models of the (112) facet considered above, the $AD_{||}$ and $AD'_{||}$ models with adatoms within the terrace and parallel dimers at the step edge were energetically more stable. Finally, the $AD_{||}$ and $AD'_{||}$ models were modified to match the experimental data by introducing a structure such as the corner hole of the DAS model at every fourth dimer site. The modified $AD_{||}$ and $AD'_{||}$ models suggest that the rows of protrusions within the (112) terrace and at the (112) step edge in the STM image originate from the adatoms and dimers, respectively. In addition, it was found that the surface states of the (112) facet have similar BEs to those of the $Si(111)-7 \times 7$ surface, even though they have different origins. This explains why the valence band structure of the $Si(557)$ surface can be similar to that of the $Si(111)-7 \times 7$ surface. Interestingly, the results suggest that both the (111) and (112) facets consist of an adatom, a dimer, and a corner hole. More interestingly, this means that the (112) facet can play a role as a 1D template, as the $Si(111)-7 \times 7$ surface has been used as a two-dimensional template for a quantum dot array.

ACKNOWLEDGMENTS

This study was supported by the Korea Research Foundation Grant funded by the Korean Government (MOEHRD)

(Grants No. KRF-2006-312-C00120 and No. KRF-2005-005-J11903) and the Korea Science Foundation through the SRC program (Center for Nanotubes and Nanostructured Composites) of MOST/KOSEF.

*ohdh@skku.edu

†jrahn@skku.edu

- ¹S. Tomonaga, Prog. Theor. Phys. **5**, 544 (1950).
- ²J. M. Luttinger, J. Math. Phys. **4**, 1154 (1963).
- ³R. E. Peierls, *Quantum Theory of Solids* (Clarendon, Oxford, 1964).
- ⁴S. C. Erwin and H. H. Weitering, Phys. Rev. Lett. **81**, 2296 (1998); J. R. Ahn, N. D. Kim, S. S. Lee, K. D. Lee, B. D. Yu, D. Heon, K. Kong, and J. W. Chung, Europhys. Lett. **57**, 859 (2002).
- ⁵H. W. Yeom, S. Takeda, E. Rotenberg, I. Matsuda, K. Horikoshi, J. Schaefer, C. M. Lee, S. D. Kevan, T. Ohta, T. Nagao, and S. Hasegawa, Phys. Rev. Lett. **82**, 4898 (1999); J. R. Ahn, J. H. Byun, H. Koh, E. Rotenberg, S. D. Kevan, and H. W. Yeom, *ibid.* **93**, 106401 (2004); G. Lee, J. Guo, and E. W. Plummer, *ibid.* **95**, 116103 (2005).
- ⁶K. N. Altmann, J. N. Crain, A. Kirakosian, J.-L. Lin, D. Y. Petrovykh, F. J. Himpsel, and R. Losio, Phys. Rev. B **64**, 035406 (2001); S. C. Erwin, Phys. Rev. Lett. **91**, 206101 (2003).
- ⁷J. R. Ahn, H. W. Yeom, H. S. Yoon, and I.-W. Lyo, Phys. Rev. Lett. **91**, 196403 (2003).
- ⁸J. R. Ahn, P. G. Kang, K. D. Ryang, and H. W. Yeom, Phys. Rev. Lett. **95**, 196402 (2005).
- ⁹S. J. Park, H. W. Yeom, J. R. Ahn, and I.-W. Lyo, Phys. Rev. Lett. **95**, 126102 (2005).
- ¹⁰R. Losio, K. N. Altmann, A. Kirakosian, J.-L. Lin, D. Y. Petrovykh, and F. J. Himpsel, Phys. Rev. Lett. **86**, 4632 (2001).
- ¹¹J. N. Crain, A. Kirakosian, K. N. Altmann, C. Bromberger, S. C. Erwin, J. L. McChesney, J.-L. Lin, and F. J. Himpsel, Phys. Rev. Lett. **90**, 176805 (2003).
- ¹²I. Barke, F. Zheng, T. K. Rügheimer, and F. J. Himpsel, Phys. Rev. Lett. **97**, 226405 (2006).
- ¹³C. Tegenkamp, Z. Kallassy, H. Pfnür, H.-L. Günter, V. Zielasek, and M. Henzler, Phys. Rev. Lett. **95**, 176804 (2005).
- ¹⁴S.-C. Li, J.-F. Jia, R.-F. Dou, Q.-K. Xue, I. G. Batyrev, and S. B. Zhang, Phys. Rev. Lett. **93**, 116103 (2004); K. Wu, Y. Fujikawa, T. Nagao, Y. Hasegawa, K. S. Nakayama, Q. K. Xue, E. G. Wang, T. Briere, V. Kumar, Y. Kawazoe, S. B. Zhang, and T. Sakurai, *ibid.* **91**, 126101 (2003); J.-L. Li, J.-F. Jia, X.-J. Liang, X. Liu, J.-Z. Wang, Q.-K. Xue, Z.-Q. Li, J. S. Tse, Z. Zhang, and S. B. Zhang, *ibid.* **88**, 066101 (2002); J. R. Ahn, G. J. Yoo, J. T. Seo, J. H. Byun, and H. W. Yeom, Phys. Rev. B **72**, 113309 (2005).
- ¹⁵A. Kirakosian, R. Bennewitz, J. N. Crain, Th. Fauster, J.-L. Lin, D. Y. Petrovykh, and F. J. Himpsel, Appl. Phys. Lett. **79**, 1608 (2001).
- ¹⁶K. Takayanagi, Y. Tanishiro, M. Takahashi, and S. Takahashi, J. Vac. Sci. Technol. A **3**, 1502 (1985).
- ¹⁷G. Kresse and J. Hafner, Phys. Rev. B **47**, 558 (1993).
- ¹⁸J. P. Perdew and A. Zunger, Phys. Rev. B **23**, 5048 (1981).
- ¹⁹P. E. Blöchl, Phys. Rev. B **50**, 17953 (1994); G. Kresse and D. Joubert, *ibid.* **59**, 1758 (1999).
- ²⁰H. J. Monkhorst and J. D. Pack, Phys. Rev. B **13**, 5188 (1976).
- ²¹S. Mankefors, Surf. Sci. **443**, 99 (1999).
- ²²J. Tersoff and D. R. Hamann, Phys. Rev. B **31**, 805 (1985).
- ²³E. D. Williams and N. C. Bartelt, Ultramicroscopy **31**, 36 (1989).
- ²⁴R. J. Phaneuf, E. D. Williams, and N. C. Bartelt, Phys. Rev. B **38**, 1984 (1988).
- ²⁵J. L. Goldberg, X.-S. Wang, J. Wei, N. C. Bartelt, and E. D. Williams, J. Vac. Sci. Technol. A **9**, 1868 (1991).
- ²⁶A. V. Zverev, Semiconductors **39**, 967 (2005).
- ²⁷I. G. Neizvestny, Surf. Sci. **600**, 3079 (2006).
- ²⁸A. N. Chaika, Semiconductors **41**, 431 (2007).
- ²⁹E. Hoque, A. Petkova, and M. Henzler, Surf. Sci. **515**, 312 (2002).
- ³⁰M. Czubanowski, A. Schuster, S. Akbari, H. Pfnür, and C. Tegenkamp, New J. Phys. **9**, 338 (2007).
- ³¹R. I. G. Uhrberg, T. Kaurila, and Y.-C. Chao, Phys. Rev. B **58**, R1730 (1998).
- ³²D. J. Chadi, Phys. Rev. B **29**, 785 (1984).
- ³³C. H. Grein, J. Cryst. Growth **180**, 54 (1997).
- ³⁴D. J. Chadi, Phys. Rev. Lett. **43**, 43 (1979).
- ³⁵K. C. Pandey, Phys. Rev. Lett. **47**, 1913 (1981).